Biosensors and Bioelectronics 26 (2011) 2781–2785

Contents lists available at ScienceDirect

Biosensors and Bioelectronics

journal homepage: www.elsevier.com/locate/bios

Short communication

Electrochemical real-time detection of L-histidine via self-cleavage of DNAzymes

Li-Dong Li*, Zheng-Bo Chen, Hong-Tao Zhao, Lin Guo*

School of Chemistry & Environment, Beijing University of Aeronautics & Astronautics, Xueyuan Rd. #37, Haidian District, Beijing 100191, China

ARTICLE INFO

Article history:
Received 8 August 2010
Received in revised form 23 October 2010
Accepted 25 October 2010
Available online 31 October 2010

Keywords:
DNAzyme
Self-cleavage
L-Histidine
Enantioanalysis
Biosensor

ABSTRACT

Herein, a rapid electrochemical biosensor for L-histidine based on highly specific, L-histidine-dependent DNAzymes is described. DNA with a single, sessile ribo-adenine, self-cleaves in the presence of L-histidine, allowing a ferrocene tag to transfer electrons to the electrode. The double-stranded DNA complex was chemi-absorbed to a gold electrode via a 3′ terminal thiol. The signal of this proposed sensor is linear over the range, 1 nM to 10 μM, with $R = 0.98775$. To improve signal intensity, gold nanoparticles were anchored to a gold electrode surface which had been previously modified with self-assembled monolayers of 1,6-hexanedithiol. With gold nanoparticle modification, a lower detection limit of 0.1 pM L-histidine and a good linear relationship over the range, 0.1 pM to 50 nM were obtained. The proposed biosensor presents high specificity for L-histidine, is not affected by the presence of other amino acids, and demonstrates excellent enantio-selectivity toward L-histidine. This proposed sensor protocol offers reasonable selectivity, rapid speed, and operational convenience for real sample assays.

1. Introduction

L-Histidine, one of the 20 natural amino acids, plays an important role as a neurotransmitter, or neuromodulator in the mammalian central-nervous system. It has also been shown to control the transport of metals in biologically important bases (Chen et al., 1999), and to minimize internal bleeding from microtrauma (Horrobin et al., 1979). Ingestion of sufficiently high levels can result in symptoms of intoxication (Liao et al., 2004). Thus, the determination of L-histidine in biological fluids may be of great importance.

The techniques most frequently used to analyze histidine levels are capillary electrophoresis (Tuma et al., 2005; Zhao and Liu, 2001; Jalali-Heravi et al., 2005; Zhang and Sun, 2004), and colorimetric (Lata et al., 2005), and fluorimetric (Li et al., 2004a,b) methods. These however, suffer from drawbacks, including unstable chemical and florescence properties, potential false signals from contaminating colorants, fluorophores and quenchers, and frequently, a reliance on cumbersome optical equipment. High performance liquid chromatography and gas chromatography with mass spectrometry have also been applied for the determination of histidine (Hovorka et al., 2002; Namera et al., 2002; Yang et al., 2005). These methods always require expensive robotic facilities and complicated operation procedures, because tedious pre-treatment of the biological sample is usually necessary. Electrochemical methods for the determination of trace amounts of histidine (Wang and Zhang, 1993; Moreira and Fogg, 1990; Zhang et al., 1995) were developed, but few papers describe the enantioanalysis of histidine. Chiral recognition has become an area of considerable interest because of its importance across the biological, chemical, and pharmaceutical sciences (Aboul-Enein and Wainer, 1997). Techniques for enantioanalysis reported to date are based on chromatography, capillary zone electrophoresis, mass spectrometry, and electroanalysis. Advantageously, electroanalysis features relatively high efficiency and low cost. However, when we compared the previous electrochemical enantioanalyses of L-histidine with our proposed method, they suffered from a shorter linear range and relatively high detection limits (Stefan-van Staden et al., 2007).

DNAzymes are catalytic DNA sequences isolated via *in vitro* selection (Breaker, 2000). Cofactor-dependent DNAzymes can often be generated by varying cofactors and cofactor concentrations during the selection process. The self-cleavage activity of RNA is due to the ribose 2′ hydroxyl. In the presence of certain cationic metals or under alkaline conditions, this hydroxyl forms a 2′ oxyanion that acts as a nucleophile in a transesterification reaction, cleaving the RNA chain. Roth and Breaker (1998) reported the *in vitro* selection of a catalytic DNA that used histidine as an active cofactor for an RNA cleavage reaction. Their kinetic analysis indicated that a DNA–histidine complex may perform a reaction analogous to the first step of the proposed catalytic mechanism of RNase A, in which the imidazole group of histidine serves as a general base catalyst. Herein, we propose an electrochemical approach to rapidly detect L-histidine on the basis of such a histidine-dependent self-cleavage DNAzyme. To the best of our knowledge, it is the first time an L-histidine biosensor based on coupling the presence of this cofactor

* Corresponding authors. Tel.: +86 010 82338162; fax: +86 010 82338162.
E-mail addresses: lilidong@buaa.edu.cn (L.-D. Li), guolin@buaa.edu.cn (L. Guo).

0956-5663/$ – see front matter © 2010 Elsevier B.V. All rights reserved.
doi:10.1016/j.bios.2010.10.041

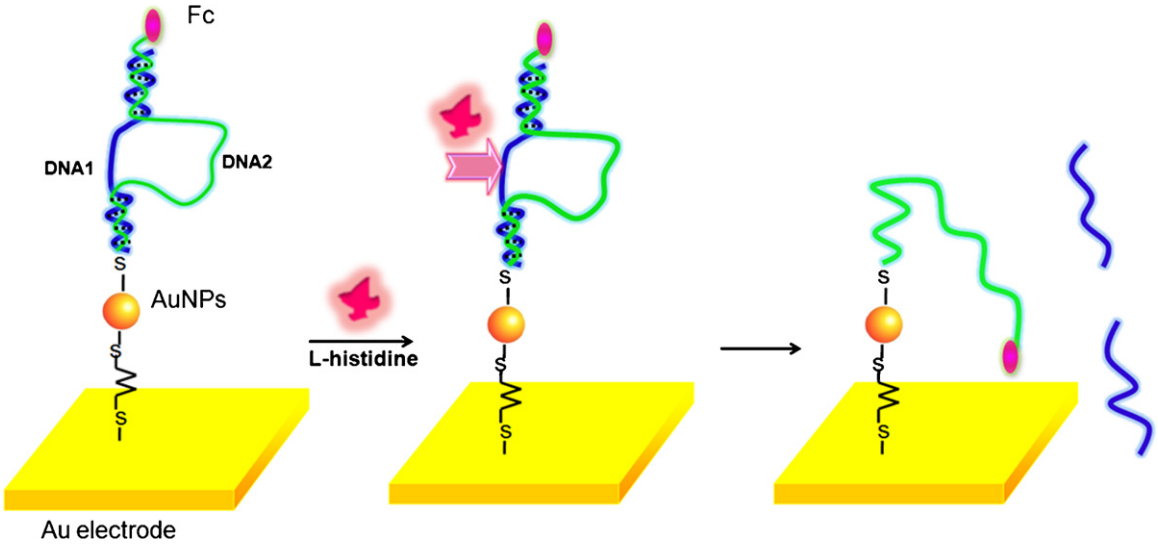

Fig. 1. Schematic diagram of the sensing mechanism for the self-cleaving DNAzyme biosensor.

with the self-cleavage activity of DNAzymes to produce sensing signals, has been proposed. The sensor demonstrated here achieves very low (0.1 pM) sensitivity and excellent selectivity, including chiral recognition, in a single, convenient step.

2. Experimental

2.1. Reagents and apparatus

The sequences of the oligonucleotides employed are as follows: DNA (1): 3′-CGA CTC ACT ATrA GGA AGA GAT G-5′, DNA (2): 3′-SH-$(CH_2)_6$-CAT CTC TTG ATC GGG GCT GTG CGG GTA GGA AGT AAT AGT GAG-5′-$(CH_2)_6$-ferrocene. The r-prefix indicates an RNA base. The above oligonucleotides were synthesized by Takara Inc. (Dalian). Cystine and valine were purchased from CNS Bioservices. 1,6-hexanedithiol (HDT, 97%) and tris-(2-carboxyethyl) phosphine hydrochloride (TCEP) were obtained from Alfa Aesar (Tianjing, China). Electrochemical measurements were performed using SWV with an electrochemical analyzer (CHI 660C, CH Instruments). A three-electrode cell consisting of a fabricated aptasensor as the working electrode, Ag/AgCl (sat. KCl) as the reference electrode and a platinum wire as the counter electrode, was employed for all electrochemical measurements. All measurements were carried out in immobilization buffer (I-B: 20 mM Tris–HCl, pH 7.41 with 140 mM NaCl, 20 mM MgCl and 20 mM KCl).

2.2. Preparation of biosensor

DNA duplexes (dsDNA) were prepared as follows: the mixture of DNA (1) and DNA (2) in I-B containing 1 mM TCEP (tris-(2-carboxyethyl)) (TCEP was employed to cleave disulfides) was heated to 90 °C and slowly cooled to room temperature. dsDNA modified gold electrodes were prepared by incubating electrodes (the bare electrode or the AuNP-modified electrode) in the thiolated dsDNA for 18 h, and thorough rinsing with I-B. For L-histidine assays, the modified electrode was placed into 2 mL histidine solutions of various concentrations. The recovery tests of the proposed biosensor towards L-histidine were checked in the presence of an artificial matrix with the following composition: 0.09% NaCl, 0.05% BSA; pH 5.5.

3. Results and discussion

3.1. Sensing mechanisms of the biosensor

The L-histidine-requiring DNAzyme we employed (DNA (1)) is a sequence-specific nuclease acting on a single-stranded DNA substrate containing a single, sessile ribo-adenine (indicated by arrow, Fig. 1). The catalytic strand (DNA (2)) is composed of a functional domain of 24 deoxynucleotides flanked by 5′ and 3′ substrate-recognition domains of 8 nucleotides each (Fig. S1). To construct signal-on architecture for a self-cleaving DNAzyme sensor, a redox probe (ferrocene) was added to the 5′ end of this strand. Thus, the proposed sensor consists of a ferrocene-modified catalytic DNA strand (2), hybridized to a complementary 22-base substrate oligonucleotide (1). To amplify the signal, gold nanoparticles ca. 15 nm diameter (Fig. S2) were first immobilized on the gold electrode surface via monolayer self-assembly (Li et al., 2010a). DNAzyme was then chemi-absorbed to the nanoparticles via a 3′ terminal thiol on the catalytic strand. In the absence of L-histidine, the duplex is relatively rigid presumably preventing the ferrocene from approaching the electrode to transfer electrons. According to predictions by the Marcus electron transfer theory, the redox reaction of ferrocene is highly distance-dependent. Therefore, at this conformation, almost no Faradic current should be observed. In the presence of L-histidine, the trans-acting catalytic strand, DNA (2), cleaves the substrate strand into two fragments at its sessile phosphodiester, the hybridization between the complementary DNA strands is presumably lost, allowing the fragments to dissociate, and releasing DNA (2) to fold into its favorable secondary configuration resulting in significant Faradaic currents, presumably because the ferrocene is in sufficiently close proximity to the electrode for electron transfer. Thus, a detectable signal is produced.

3.2. Characterization of biosensor

To clarify the electrochemical properties of the proposed sensor, cyclic voltammogram (CV) and electrochemical impedance spectroscopy (EIS) were employed to monitor each step of fabrication. As shown in Fig. S3(A), at the bare gold electrode, the $Fe(CN)_6^{3-}$ redox couple showed reversible behavior with peak-to-peak separation, ΔE_p, of 78 mV (Fig. S3(A), curve a). After 1,6-hexanedithiol (HDT) was self-assembled onto the gold electrode, the CV shape

changed dramatically, consistent with electrode passivation caused by a well-packed HDT monolayer (Fig. S3(A) curve b). After colloidal AuNP immobilization on the HDT-modified gold electrode, the reversibility of the AuNP/HDT/gold electrode was markedly improved with a ΔE_p of 65 mV, compared with 78 mV of the bare gold electrode. The peak current (I_a = 13.3 μA) also surpassed that for the bare gold electrode (I_a = 13.0 μA) (Fig. S3(A), curve c), suggesting that the electron transfer process blocked by HDT was restored by the AuNP layer, and indicating that AuNPs accelerate electron transfer between the redox marker and electrode surface. After DNAzyme immobilization on the surface of the AuNP/HDT/gold electrode, the electrode exhibited a significant increase in ΔE_p (value, 281 mV), probably due to the kinetics barrier created between $[Fe(CN)_6]^{3-/4-}$ and the negatively charged DNA phosphate backbones (Fig. S3(A) curve d).

The process above was confirmed by EIS, as shown in Fig. S3(B). The change in semicircle diameter results from changes in interfacial resistance, Ret, due to electrons transferring from the modified electrode to $[Fe(CN)_6]^{3-/4-}$ in solution. Curve a represents the electrochemical impedance of the bare gold electrode, which is approximately linear. After HDT modification, the diameter of the semicircle increased dramatically with a Ret of 1.72×10^7 Ω (inset of Fig. S3(B)). After AuNP self-assembly on the HDT-modified electrode, the electrochemical response was again approximately linear (Fig. S3(B), curve b), similar to curve a, indicating that AuNPs restore the electron transfer rate. After DNA duplexes were immobilized onto the AuNP/HDT/gold electrode, the Ret significantly increased to 1.96×10^4 Ω (Fig. S3(B), curve c). This can be attributed to the fact that $[Fe(CN)_6]^{3-/4-}$ received electrostatic repulsive forces from the negatively charged DNA phosphate backbones

3.3. Packing density of DNA probes

The signal of an electrochemical biosensor depends on the amount of probe on the electrode (Peterson et al., 2002). The packing densities of DNAzymes immobilized on both a bare electrode, and on one coated with gold nanoparticles were measured by electrochemical methods (Yu et al., 2003). By our experiments (Fig. S4), the surface coverage of the DNAzymes (1) was estimated at 4.3×10^{11} molecules cm^{-2} and 1.0×10^{12} molecules cm^{-2}, on the bare Au electrode and the AuNP-modified gold electrode, respectively (Li et al., 2010b). The active surface areas of a bare Au electrode and an AuNP-modified Au electrode were measured by CV in 0.5 M H_2SO_4 (Fig. S5). Assuming a specific charge of 386 μC/cm^2 is required for gold oxide reduction (Szamocki et al., 2007), the bare Au electrode had a total active surface of 4.7×10^{-2} cm^2, whereas that of the AuNP-modified electrode was 1.3×10^{-1} cm^2, indicating that the active electrode surface area had been enlarged approximately 2.8 times by AuNP modification. Therefore, the total amount of immobilized DNAzymes would be 2.0×10^{10} molecules and 1.3×10^{11} molecules, for the bare elec-

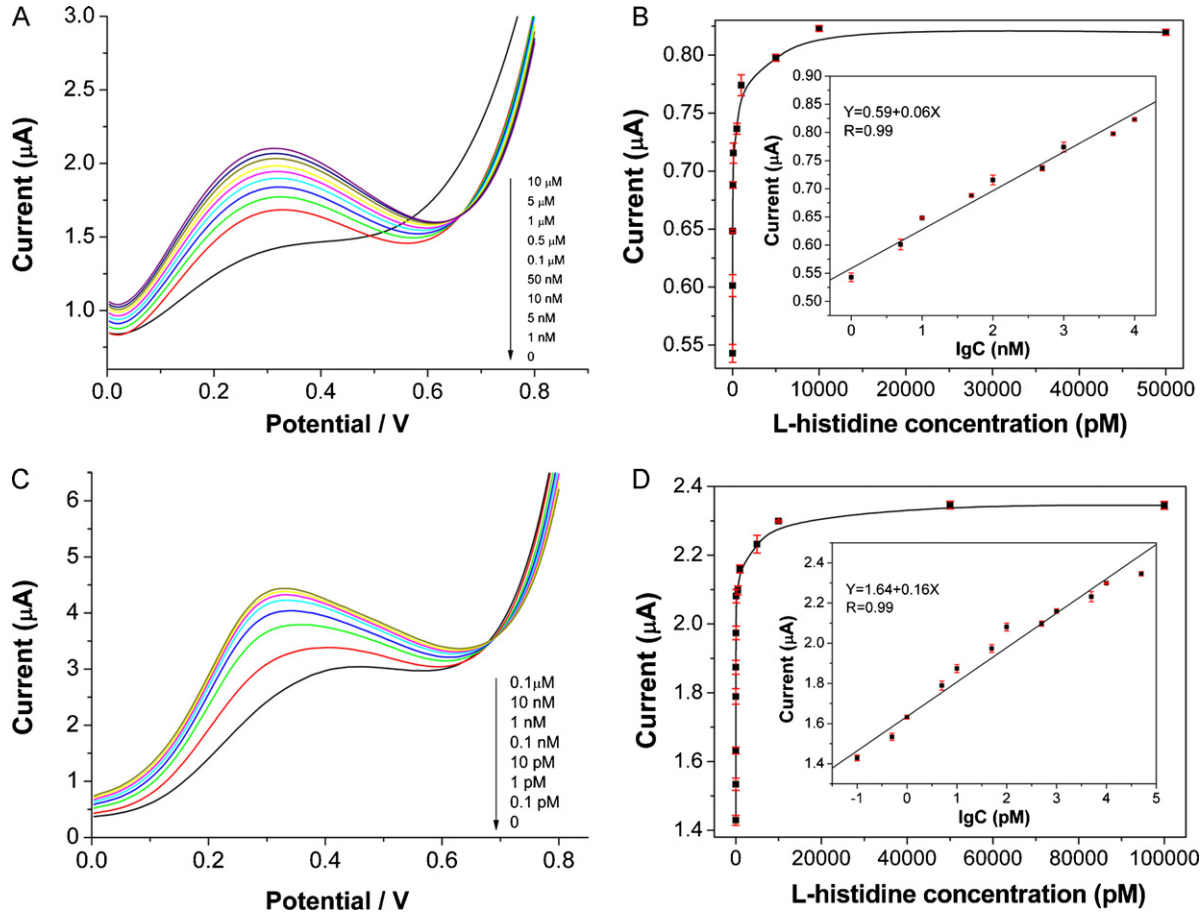

Fig. 2. Square-wave voltammogram measurement of both DNA duplex/Au electrode and DNA duplex/AuNP/HDT/Au electrode. (A) Square-wave voltammograms of DNA duplex/Au electrode to different concentrations of L-histidine. (B) The peak current in the SWV as a function of L-histidine concentration. Inset: the SWV peak current is linear with logarithm of L-histidine concentration over the range from 1.0×10^{-9} to 1.0×10^{-5} M. (C) Square-wave voltammograms of DNA duplex/AuNP/HDT/Au electrode to different concentrations of L-histidine. (D) The peak current in the SWV as a function of L-histidine concentration. Inset: the SWV peak current is linear with logarithm of L-histidine concentration over the range from 1.0×10^{-13} to 5.0×10^{-8} M. The illustrated error bars represent the standard deviation of three measurements conducted with a single electrode at each concentration.

Table 1
Relative standard deviations at specific concentrations of L-histidine.

Using duplex/gold electrode ($n=3$)									
C (nM)	1	5	10	50	100	500	1000	5000	10,000
RSD	1.4%	1.6%	0.2%	0.4%	1.2%	0.6%	1.2%	0.4%	0.3%

Using DNA duplex/AuNP/HDT/Au electrode ($n=3$)												
C (pM)	0.1	0.5	1	5	10	50	100	500	1000	5000	10,000	50,000
RSD	0.4%	0.5%	0.2%	0.4%	0.1%	0.5%	0.1%	0.2%	0.1%	0.2%	0.1%	0.2%

trode and the AuNP-modified electrode, respectively, a 6.5-fold increase. Thus the proposed sensor with AuNP modification could detect more target molecules, enhancing the signal response.

3.4. SWV measurement of L-histidine

The self-cleaving DNAzyme-based sensor is sensitive and specific to its target molecule. In order to test signal enhancement for DNAzymes with AuNP modification, square wave voltammetry (SWV) was carried out at both the duplex/gold electrode and the duplex/AuNP/HDT/gold electrode. Fig. 2(A) depicts SWV profiles for the bare electrode with DNA duplex modification after reacting with concentrations of L-histidine from 1 nM to 10 μM. In the absence of L-histidine, only a very tiny Faradaic current was observed at 0.3 V due to the redox reaction of ferrocene. We presume this residual peak arises because the surface-immobilized Ferrocene-tagged DNA (2) strand is in conformational equilibrium between a duplex DNA and its favorable bent-over secondary configuration. Upon increasing L-histidine, we observed a large increase in Faradaic current. The directly measured detection limit is 1 nM, and the SWV current is approximately linear over the range, 1 nM to 10 μM (Fig. 2(B)). In contrast, Fig. 2(C) shows the SWV profiles for the duplex/AuNP/HDT/gold electrode. The detection limit has greatly decreased to 0.1 pM, and the signal is linear over the range, 0.1 pM to 50 nM (Fig. 2(D)). Thus, gold nanoparticle modification lowers the detection limit by 4 orders of magnitude. This is consistent with an increase in the amount of DNAzymes immobilized. Of note, as shown in Fig. 2(C), the oxidative peak potential of ferrocence shifts negatively with increasing concentration of L-histidine, which can be ascribed to the positively charged nature of the amino acid. The relative standard deviation for results from the DNA duplex/gold electrode and DNA duplex/AuNP/HDT/gold electrode for each L-histidine concentration, are listed in Table 1. These indicate that the proposed biosensor offers excellent reproducibility (RSDs < 1.6%, $n=3$).

3.5. The response time of biosensor

The sensor equilibrates rapidly. We observed a 98% total signal change within 28 s, and complete saturation in less than half a minute (Fig. S6). Therefore, it can serve as a real-time sensor for the detection of L-histidine. In our experiments, after the fabricated sensor had been inserted into the L-histidine sample solution, measurements were taken in 30 s. We presume the fast response was due to the high catalytic activity of the DNAzyme with $k_{obs} = 0.2\ min^{-1}$ (23 °C, pH 7.5) (Roth and Breaker, 1998), and the fast equilibrium between the duplex configuration and the favorable secondary structure of the DNA (2). Generally, the dependence of the rate constant of self-cleaving DNAzymes on temperature follows the Arrhenius equation, increasing approximately linearly with temperature and reaching a maximum at 37 °C. For convenience, all our L-histidine assays were carried out at room temperature.

3.6. The specificity of biosensor

The specificity of the proposed biosensor was determined by challenging it with a mixture of two similar amino acids, each at 1 mM concentration. As shown in Fig. 3(A), no significant signal change was observed for amino acids other than L-histidine. We also performed enantioanalysis of histidine. As shown in Fig. 3(B), no signal was observed with D-histidine even at a very high concentration of 1 mM. After the addition of 1 nM L-histidine, a significant enhancement of the signal was obtained, indicating perfect chiral selectivity for this proposed sensor. This enantio-selectivity is due to the good chiral specificity of L-histidine DNAzymes (Roth and Breaker, 1998).

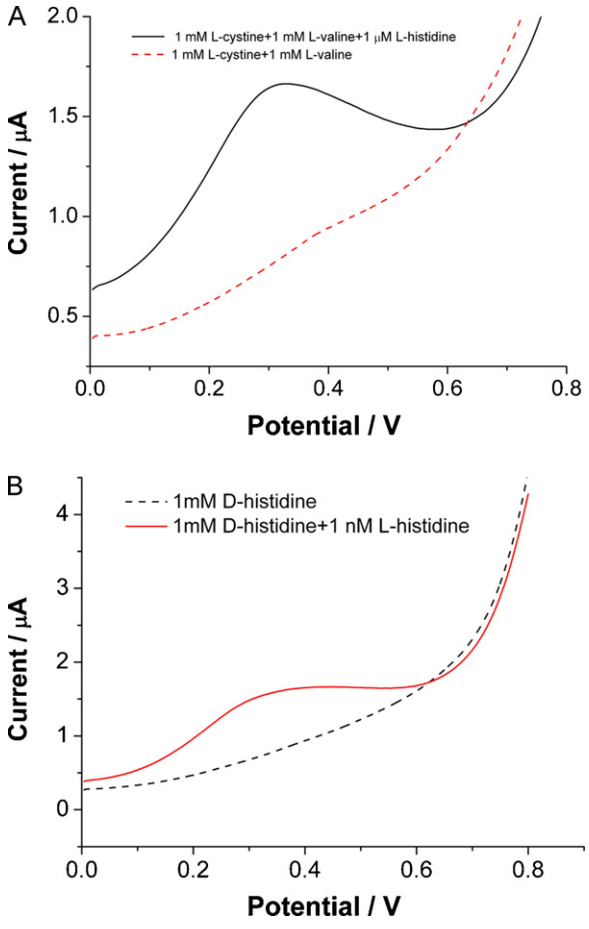

Fig. 3. Specificity detection of the sensing system. (A) Square-wave voltammograms for the DNA duplex/Au electrode after reacting with a mixture of 1.0×10^{-6} M L-histidine, 1.0×10^{-3} M cystine and 1.0×10^{-3} M valine (solid line) and a mixture of 1.0×10^{-3} M cystine and 1.0×10^{-3} M valine (dashed line). (B) Square-wave voltammograms for the DNA duplex/Au electrode after reacting with a mixture of 1.0×10^{-9} M L-histidine and 1.0×10^{-3} M D-histidine (solid line) and 1.0×10^{-3} M D-histidine (dashed line).

3.7. Real sample analysis

To investigate if the method was applicable to real samples, we tested an artificial physiological matrix and spiked samples with different L-histidine concentrations. The recoveries of standard addition were 97.772%, 99.608%, 99.393% and 99.574% for L-histidine concentrations of 5 nM, 50 nM, 0.5 μM, and 5 μM respectively, when using the DNA duplex/gold electrode. We consider that blood serum samples would require dilution to 10^{-10} M and to 10^{-7} M, for the AuNP-modified electrode and the bare electrode, respectively (normal blood serum level 0.31–26.35 μg/m) (Prasad et al., 2009). This large dilution is helpful to diminish false-positive contributions from the matrix.

4. Conclusions

In this study, novel reagentless signal-on architecture was designed for the detection of L-histidine, in which a self-cleaving DNAzyme was used as a molecular recognition element, and Ferrocene as a redox tag. To improve sensitivity, 15 nm AuNPs were applied to the gold electrode surface via a self-assembled HDT monolayer. A detection limit of 0.1 pM was achieved by this gold nanoparticle modification. The self-cleaving DNA-based electronic sensor described here exhibits excellent sensitivity and specificity and chiral selectivity for its target molecule. It allows rapid detection with operational convenience. Given the potential for *in vitro* selection to supply cofactor-dependent self-cleaving DNAzymes, and given that it appears that DNAzymes can be immobilized without loss of activity; this approach may prove of general utility for electrochemical analyte detection.

Acknowledgements

This project was financially supported by The National Natural Science Foundation of China (nos. 20903008, 20973019, and 50725208) and The State Key Project of Fundamental Research for Nanoscience and Nanotechnology (2006CB932300). The authors thank M. Wyatt for comments on the manuscript.

Appendix A. Supplementary data

Supplementary data associated with this article can be found, in the online version, at doi:10.1016/j.bios.2010.10.041.

References

Aboul-Enein, H.Y., Wainer, I.W. (Eds.), 1997. The impact of stereochemistry on drug development and use. John Wiley and Sons, New York.
Breaker, R.R., 2000. Science 290, 2095–2096.
Chen, G.N., Wu, X.P., Duan, J.P., Chen, H.Q., 1999. Talanta 29, 319–330.
Horrobin, D.F., Mandu, M.S., Oka, M., Morgan, R.O., Cunnane, S.C., Aly, A.I., Ghayur, T., Schweitzer, M., Karmali, R.A., 1979. Med. Hypothesis 5, 969.
Hovorka, S.W., Williams, T.D., Schoneich, C., 2002. Anal. Biochem. 300, 206–211.
Jalali-Heravi, M., Shen, Y., Hassanisadi, M., Khaledi, M.G., 2005. Electrophoresis 26, 1874–1885.
Lata, S., Reichel, A., Brock, R., Tampe, R., Piehler, J., 2005. J. Am. Chem. Soc. 127, 10205–10215.
Liao, H.P., Zhang, Z.H., Nie, L.H., Yao, S.Z., 2004. J. Biochem. Biophys. Methods 59, 75–87.
Li, L.D., Chen, Z.B., Zhao, H.T., Mu, X.J., Guo, L., 2010a. Sens. Actuators B 149, 110–115.
Li, L.D., Zhao, H.T., Chen, Z.B., Mu, X.J., Guo, L., 2010b. Anal. Bioanl. Chem. 398, 563–570.
Li, X.H., Ma, H.M., Nie, L.H., Sun, M., Xiong, S.X., 2004a. Anal. Chim. Acta 515, 255–260.
Li, X.H., Ma, H.M., Dong, S.Y., 2004b. Talanta 62, 367–371.
Moreira, J.C., Fogg, A.G., 1990. Analyst 115, 41–43.
Namera, A., Yashiki, M., Nishida, M., Kojima, T., 2002. J. Chromatogr. B 776, 49–55.
Peterson, A.W., Wolf, L.K., Georgiadis, R.M., 2002. J. Am. Chem. Soc. 124, 14601–14607.
Prasad, B.B., Srivastava, S., Tiwari, K., Sharma, P.S., 2009. Mater. Sci. Eng. C 29, 1781–1789.
Stefan-van Staden, R.-I., Lal, B., Holo, L., 2007. Talanta 71, 1434–1437.
Roth, A., Breaker, R.R., 1998. Proc. Natl. Acad. Sci. U.S.A. 95, 6027–6031.
Szamocki, R., Velichko, A., Holzapfel, C., 2007. Anal. Chem. 79, 533–539.
Tuma, P., Samcova, E., Balinova, P., 2005. J. Chromatogr. B 821, 53–59.
Wang, L.Z., Zhang, X.L., 1993. Chin. J. Anal. Chem. 21, 569.
Yang, Z.P., Hancock, W.S., Chew, T.R., Bonilla, L., 2005. Proteomics 5, 3353–3366.
Yu, H.Z., Luo, C.Y., Sankar, C.G., Sen, D., 2003. Anal. Chem. 75, 3902–3907.
Zhang, L.Y., Sun, M.X., 2004. J. Chromatogr. A 1040, 133–140.
Zhang, X.L., Ma, C.S., Deng, L.A., 1995. Chin. J. Anal. Chem. 6, 783.
Zhao, S., Liu, Y.M., 2001. Anal. Chim. Acta 426, 65–70.